Creation of Laguerre-Gaussian laser modes using diffractive optics

Sharon A. Kennedy, Matthew J. Szabo, Hilary Teslow, James Z. Porterfield, and E. R. I. Abraham
University of Oklahoma, Department of Physics and Astronomy, 440 West Brooks Street, Norman, Oklahoma 73019
(Received 16 April 2002; published 4 October 2002)

Diffractive optics are used to create low- and high-order Laguerre-Gaussian (LG) beams from the output of a diode laser. We examine the mode purities, conversion efficiencies, extinction ratios, and propagation characteristics. We present detailed analyses of the beam profiles for one low-order (LG_0^1) and one high-order (LG_1^2) Laguerre-Gaussian mode. Modeling the LG_1^2 beam as a superposition of LG modes, we find (99.3 $\pm 0.9\%$) of the laser intensity in the LG_1^2 mode, a mode purity greater than for LG beams created by other methods external to the laser cavity. The high mode purity may be useful in making atom traps for precision measurements and for Bose-Einstein condensation.

DOI: 10.1103/PhysRevA.66.043801 PACS number(s): 42.60.Jf, 32.80.Pj, 42.50.Vk

Laser beams propagating in Laguerre-Gaussian modes are of considerable interest due to their characteristic phase singularity, orbital angular momentum, and multiply connected topology. Laguerre-Gaussian beams (LG_p^ℓ) describe a set of propagation modes where the equation for the radial electric field is proportional to the product of a Gaussian and an associated Laguerre polynomial L_p^ℓ. When ℓ is greater than zero, the electric field has an azimuthal phase change of $2\pi\ell$, which results in a phase singularity in the field and a node in the intensity at the center of the beam.

These beams are used as optical tweezers for macroscopic particles, where the transfer of orbital angular momentum leads to rotation in a direction determined by the helicity of the beam [1,2]. LG beams are used to write optical waveguides in atomic vapors [3], and the vortex nature of these beams is exploited in the study of optical solitons [4]. These types of laser modes also produce atom traps. Magneto-optical traps (MOT's) have been demonstrated using a combination of LG_0^1 (donut-mode) beams and very weak Gaussian beams [5]. The construction is similar to a traditional MOT with the exception that the light intensity at the center is much weaker. This leads to an increase in the number of trapped atoms due to a decrease in collisions between ground-state and excited-state atoms that lead to trap loss. LG beams are also used for optical dipole traps [6]. In a dipole trap, a laser tuned to a frequency lower than an atomic resonance transition frequency (red detuned) attracts atoms to the region of maximum light intensity, while a laser tuned above resonance (blue detuned) attracts atoms to minimum intensity regions. Blue-detuned dipole-force traps constructed from LG beams confine atoms to the nodes in intensity where they spend most of the time in the dark. This arrangement can trap a larger number of atoms than that achieved with traditional red-detuned dipole-force traps [6]. Confining atoms in the intensity nodes minimizes effects such as photon absorption and ac Stark shifts, which is important for precision measurements. While previous experiments confine atoms in the center of a donut-mode beam, there is considerable interest in high-order LG beams as toroidal traps for Bose-Einstein condensates [7,8]. Confinement of multiple condensates in the concentric, multiply connected traps formed by high-order LG modes allows observation of vortices by matter-wave interference [8].

For a laser beam propagating along the z axis, the magnitude of the electric field of an LG_p^ℓ mode (setting $z=0$ and assuming a planar wave front) is given by [9]

$$u_p^\ell(r,\phi) = \sqrt{\frac{2P}{\pi w^2}}\sqrt{\frac{p!}{(l+p)!}}(-1)^p e^{-i\ell\phi} e^{-r^2/w^2} \times \left(\frac{\sqrt{2}r}{w}\right)^\ell L_p^\ell\left(\frac{2r^2}{w^2}\right), \quad (1)$$

where P is the power, w is the laser beam waist (which is a function of z), and L_p^ℓ is a Laguerre polynomial that gives the characteristic $p+1$ radial nodes. The $e^{-i\ell\phi}$ term identifies this as a vortex state with a quantized $2\pi\ell$ azimuthal phase change of the electric field, and a well-defined angular momentum of $\ell\hbar$ per photon [10]. When $\ell=p=0$, the beam is Gaussian. Figure 1 contains sample charge-coupled device (CCD) camera images of cross sections of LG beam intensities (given by u^*u) and shows the qualitative features of the intensity distributions for several modes.

While LG modes can be produced inside the laser cavity [11], or by subsequent conversion from Hermite-Gaussian beams [10,12], the use of diode lasers requires external-cavity conversion from Gaussian to LG propagation modes. Previously demonstrated external-cavity methods include spiral phase plates, computer generated holograms, and diffractive optics. Spiral phase plates are transmission optics whose thickness varies to create an azimuthally dependent phase delay. This can convert a Gaussian beam into a LG_p^ℓ beam, as well as convert between any two LG_p^ℓ modes [13,14]. A more common method uses computer generated holographic gratings [15–17]. Computer generated holograms are recordings of the theoretical interference pattern between the electric field of the LG mode of interest and a reference field, commonly a plane wave [18]. Most studies using computer generated holograms transform Gaussian beams into LG_0^ℓ, donut modes. For $p=0$, an incident Gaussian beam is broken into diffractive orders, the LG_0^ℓ beam being in the ℓth diffractive order. The gratings are designed to put optimum power in the desired mode, achieved with conversion efficiencies of $\sim 40\%$ [16]. While higher-order, $p\neq 0$, modes have been demonstrated using computer gen-

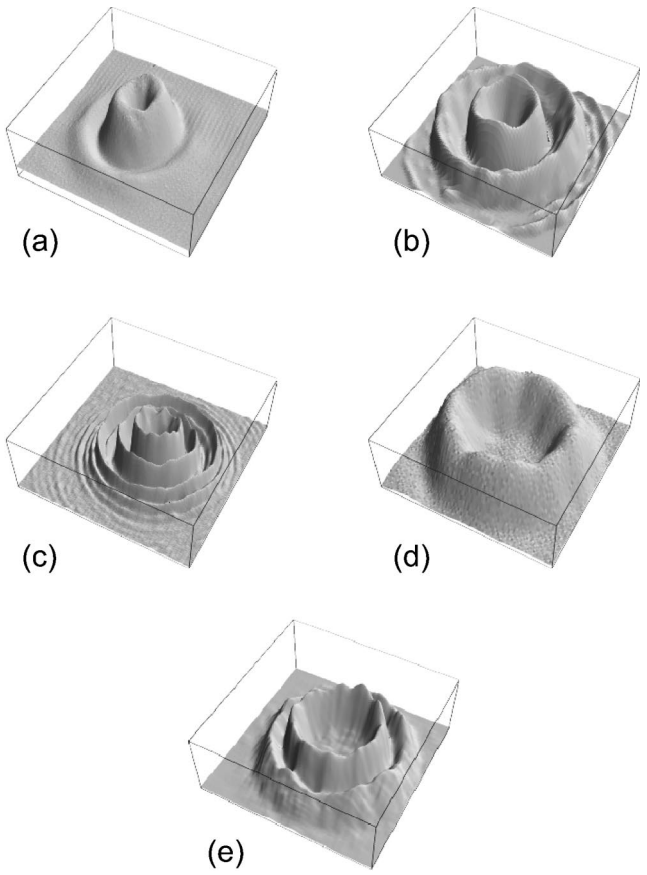

FIG. 1. Two-dimensional (2D) intensity profiles of LG_p^ℓ beams: (a) LG_0^1, (b) LG_1^2, (c) LG_2^3, (d) LG_0^5, and (e) LG_1^{10}. The additional rings seen in (a)–(c) are due to diffraction from the edge of the optic.

erated holograms [16], they cannot create pure LG modes. In this case, each diffractive order of a specific ℓ is a superposition of all p modes. Arlt *et al.* [16] show that the theoretically best possible mode purity for a LG_1^1 beam has 80% of the intensity in the p mode of interest. They achieve this experimentally with a conversion efficiency of 40%.

We constructed Laguerre-Gaussian laser beams using diffractive optics in collaboration with the research department of Diffractive Optics Corporation (DOC). DOC uses state-of-the-art photolithographic techniques to etch small scale structures on an optical element. A laser wave front incident on the optic diffracts from the microstructures. These new wave fronts propagate, and the resulting beam profile is the superposition of the diffracted waves. Using two diffractive optics to control the intensity and the phase, an arbitrary final wave front can be created at a specific propagation distance from the second optic, given an arbitrary initial wave front. There is no fundamental limit to the mode purity of beams created with this method; it is only limited by the resolution of the lithographic techniques used to etch the diffractive optics. Using these optics we created LG_0^1, LG_1^2, LG_2^3, LG_0^5, and LG_1^{10} laser modes. Images of intensity cross sections for these beams are pictured in Fig. 1. Khonina *et al.* have also made diffractive optics to generate Laguerre-Gaussian laser beams, and they present CCD images of the beams in Ref. [19].

500 mW of single-frequency laser power at 780 nm is produced by an external-cavity diode laser and amplifier in the master oscillator power amplifier (MOPA) configuration. The astigmatic output of the MOPA is symmetrized by beam shaping optics and passed through an optical diode to prevent back reflections. The beam is inserted into a single-mode fiber to spatially filter the beam, and we routinely obtain ~ 10 mW of laser light exiting the fiber in a pure Gaussian laser mode. Since very little power is required for these studies, we do not optimize the coupling into the fiber. With a telescope, we produce a collimated beam with an e^{-2} beam radius of 0.5 mm set by the size of the etched portion of the optics. The beam is directed through two diffractive optics held on either end of a specially designed mount. The mount is a hollow aluminum cylinder, 15 mm long, 25.4 mm outer diameter, and 12.7 mm inner diameter, through which the beam passes. On each face of the cylinder are pins to fix the orientation of the optics. This cylinder is placed in a 1 in. optic mount and fixed to a 2D translation stage, which together allow control of both the position and angle of the optics relative to the laser beam. These optics must be placed 15.0 ± 0.2 mm apart and have a relative tilt angle of less than ± 3 arc min along any axis. These specifications were determined by DOC, and the orientation must be optimized for best mode purity. The optics are designed to create the desired image 15 mm from the second optic and have a wavelength range of ± 10 nm.

Samples of unoptimized beams showing the general features of LG_p^ℓ modes are in Fig. 1, where the images are taken using a low-resolution CCD camera in conjunction with a frame grabber and PC coordinated through LABVIEW. The intensity scale is in arbitrary units. Figures 1(a) and 1(d) are images of the LG_0^1 and LG_0^5 beams, each showing the expected one central node. The node of the LG_0^5 beam is qualitatively different from that of the LG_0^1 beam, since the intensity at the center of a LG_p^ℓ mode scales as $r^{2\ell}$ [Eq. (1)]. Figures 1(b) and 1(e) are images of the LG_1^2 and LG_1^{10} beams, each with one $r \neq 0$ node in addition to the center node. Once again, there is a proportionally larger region of near-zero intensity at the center of the LG_1^{10} beam. As also seen in the figure, for each set of modes with the same p, but different ℓ, the width of the annular intensity ring is narrower for the beam with higher ℓ. Consequently, the peak intensity is larger. Figure 1(c) is an image of a LG_2^3 laser beam with multiple $r \neq 0$ nodes. Figures 1(a)–1(c) show additional rings around the outside of the beams and are due to diffraction from the outer edge of the optic. These extra rings diverge very quickly as the LG beam propagates and are no longer observed further down the beam path.

The conversion efficiency, the ratio of the power in the LG mode of interest to the power of the incoming Gaussian beam, is a figure of merit for LG beam creation. In principle, LG modes created intracavity or by using high-order Hermite-Gaussian modes do not suffer from conversion losses in this sense. However, the requirement that the laser operate in a higher mode decreases gain. A comparable figure of merit for these systems would be the ratio of LG mode power to the power possible in the fundamental mode of the

laser. Computer generated holograms have a demonstrated conversion efficiency of 78% for LG_0^1 [16] and 40% for higher-order beams. Using a power meter before and after the diffractive optics, we measure conversion efficiencies of greater than 40% for our LG_0^1 beam and greater than 60% for the higher-order modes.

A primary consideration for methods of LG beam construction is the resulting mode purity: the degree to which the intensity pattern reproduces the theoretical mode. This becomes an important issue for $p \neq 0$ beams made from computer generated holograms because beams that correspond to a particular value of ℓ are a superposition of all p values. To quantify this, Arlt *et al.* [16] took the total intensity in the diffraction order of interest and measured the percentage of the intensity in the specific p mode desired. They fitted the intensity distribution to a function given by f^*f, where $f = \Sigma_p c_p u_p^\ell$, u_p^ℓ is given by Eq. (1), and c_p are numerical coefficients. The figure of merit is then $c_{p_o}^2$, where p_o is the desired mode. They fitted data for LG_1^1 beams using amplitude terms up to $p=3$. They were able to obtain a LG_1^1 beam with $c_1^2 \simeq 0.8$, matching the maximum theoretical value for beams created with computer generated holograms [16].

An accurate radial intensity distribution is necessary to determine the mode purity. We first create the beams as described above. Then, to optimize the beam quality, we place a CCD camera near the optimum image plane and adjust the position and angle of the optics to improve the observed image. Because the CCD camera does not provide sufficient signal to noise, we use a 10 μm pinhole on a translation stage to measure the intensity. We place the pinhole in the optimum image plane of the optics and focus the transmitted light onto a photodiode with amplifier circuit. We find the positions corresponding to the maximum intensity of the LG beam both vertically and horizontally, and the center is taken to be the midpoint between these positions. We obtain a 1D intensity versus radius distribution by measuring the output of the photodiode circuit with the pinhole starting at the center of the beam and moving radially outward. The background due to scattered laser light and ambient room light is found and subtracted from the data. We find that the dominant sources of errors are introduced into the experiment in the initial setup; including uncertainties in alignment optimization, placing the pinhole at the image plane, and determining the center of the beam. To randomize these errors, we make many independent alignments and measurements of the intensity distribution, and compute the average and standard deviation at each position. Figure 2 shows the measured radial intensity distribution for the LG_1^2 beam, and Fig. 3 shows the data for the LG_0^1 beam.

To compute a figure of merit for our mode purity, we analyze our data in a manner similar to that of Ref. [16] by fitting to a superposition of p modes and minimizing χ_ν^2, the reduced χ^2 [20]. Even though we do not expect our beams to be a superposition of p modes, we let nonzero amplitudes of the other p modes account for any systematic errors. Using MATHEMATICA, we begin by fitting our data to a pure LG_p^ℓ mode, plotting contours of χ_ν^2, and finding the minimum. If the result is greater than 1, we add another term in the expansion and again minimize χ_ν^2. We continue to add terms until χ_ν^2 no longer decreases. For each fit we require $\Sigma_p c_p^2 = 1$. We find quantitatively that this model is a good choice for our data as the final χ_ν^2 is nearly 1. Then, as in Ref. [16], the mode purity is given by $c_{p_o}^2$ of the desired p_o mode. Using this method, we find the mode purity of the LG_1^2 beam to be $c_1^2 = 0.993 \pm 0.009$, consistent with 100% of the beam intensity being in the LG_1^2 mode. For the LG_0^1 beam, $c_0^2 = 0.929 \pm 0.125$. The theoretical curves that best fit the data are shown as lines in Figs. 2 and 3.

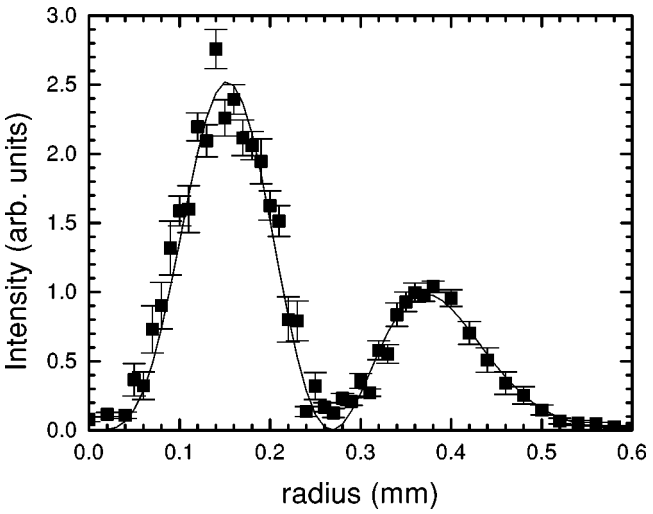

FIG. 2. The squares are experimental measurements of the radial intensity of a LG_1^2 beam with the error bars representing one standard deviation. The line is the theoretical curve that best fits the data showing >99% of the beam intensity in the LG_1^2 mode.

Because an advantage to trapping atoms in blue-detuned laser fields is that they spend most of the time in regions of low laser intensity, an important quality of LG beams is how

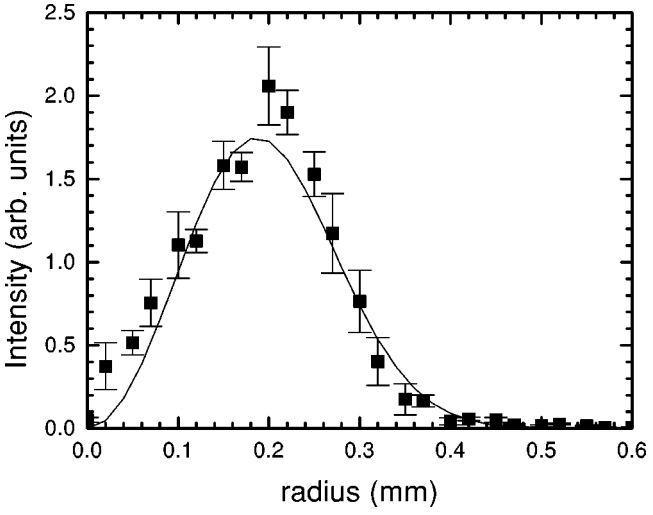

FIG. 3. The squares are experimental measurements of the radial intensity of a LG_0^1 beam with the error bars representing one standard deviation. The line is the theoretical curve that best fits the data showing >92% of the beam intensity in the LG_0^1 mode.

TABLE I. Comparison of LG_p^ℓ beam characteristics using different construction methods.

Creation method	ℓ mode	Mode purity $p=0$	Mode purity $p=1$	Conversion efficiency	Extinction ratio
Spiral phase plate	1	78.5% [14]			
	2	50% [14]			
Computer generated	1	93% [17]	80% [16]	40%	
holograms	3	77% [17]			
	6	62.8% [17]			
Diffractive optics	1	92.9%		40%	$(2.5\pm0.8)\times10^{-2}$
(this work)	2		99.3%	60%	$(3.3\pm0.8)\times10^{-2}$

dark the nodes are. A figure of merit of this characteristic is the extinction ratio: the ratio of the peak intensity to the intensity at the center. We measure extinction ratios of $(3.3\pm0.8)\times10^{-2}$ for the LG_1^2 beam and $(2.5\pm0.8)\times10^{-2}$ for the LG_0^1 beam. In fact, as seen in Figs. 2 and 3, our beams vary from the theoretical curve mostly where the intensity is supposed to go to zero. This may be a concern for some applications, such as precision measurements. To our knowledge a study of the extinction ratios of LG beams obtained by other methods has not been done, and would be of considerable interest. Table I shows a comparison of our results with the available data published on LG modes created using methods external to the laser cavity.

To further explore the practical application of these beams as atom traps, we consider their propagation characteristics. Although the initial beam is transformed through diffraction over 30 mm, the resulting LG modes maintain their qualitative shape over significant distances due to the vortex nature of the beams. Figure 4 shows a LG_0^1 beam at various distances from the image plane. The beam diverges as it propagates, and there is some distortion in the beam quality. At 75 mm [Fig. 4(a)], there is a prominent extra ring around the central node. This is due to light diffracting from the outer edge of the optic itself, similar to that observed in Figs. 1(a)–1(c). These diffraction rings diverge more rapidly than the LG beam, and at 200 mm the extra ring is no longer visible. The general feature of an LG_0^1 beam, the central node, is maintained as the beam propagates. Figure 5 shows CCD images of a LG_2^3 beam as it propagates from the image plane. Again, as the beam diverges, the multiple radial nodes of the beam are preserved. The relative peak intensities of the antinodes change as a function of propagation distance. Additionally, an azimuthal asymmetry in peak intensity appears, and then increases as the beam propagates. While the mode purity can be recaptured by imaging, it may not be necessary if only general features of the beam are required.

We use diffractive optics to create low- and high-order Laguerre-Gaussian diode laser beams with mode purities

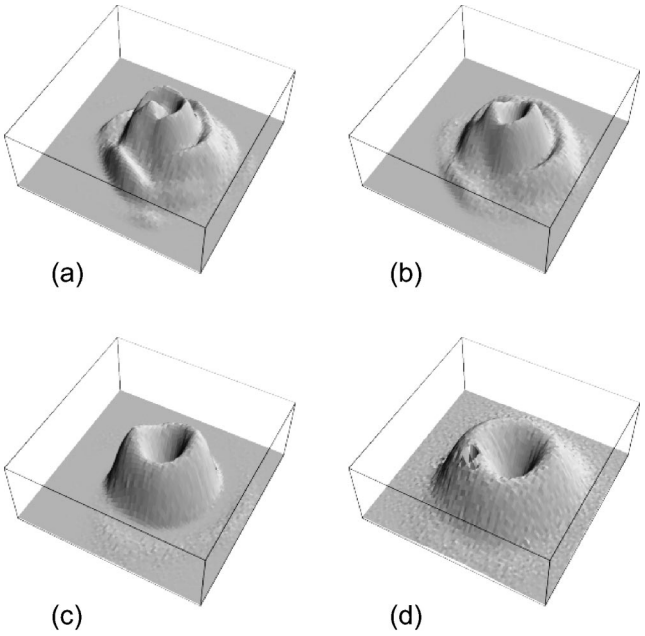

FIG. 4. Images of a LG_0^1 beam at increasing distances from the image plane: (a) 75 mm, (b) 100 mm, (c) 150 mm, and (d) 200 mm. The dimple in (d) is an experimental artifact. The additional ring in (a)–(b) is due to diffraction from the edge of the optic.

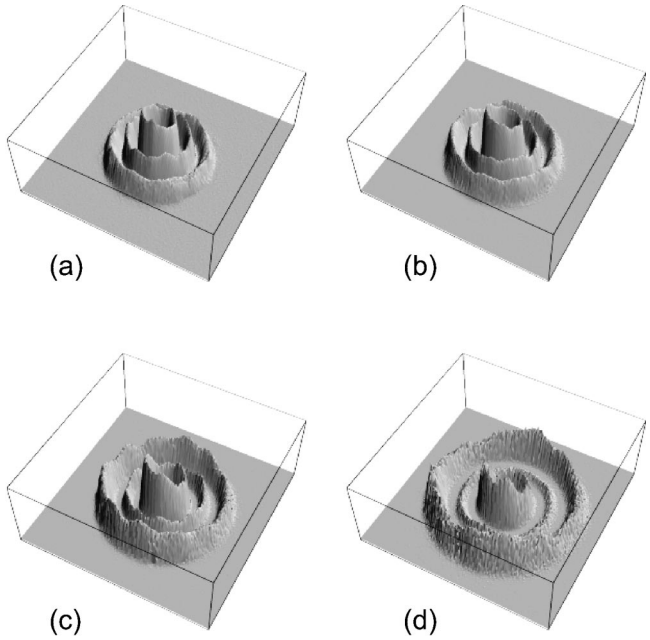

FIG. 5. Images of a LG_2^3 beam at increasing distances from the image plane: (a) 75 mm, (b) 100 mm, (c) 150 mm, and (d) 200 mm.

greater than 90%, superior to those of other external-cavity methods. The beams have conversion efficiencies comparable to those in other techniques and extinction ratios of $\sim 10^{-2}$. The beams maintain their qualitative features over distances greater than 200 mm from the image plane of the optics. Because of the good mode purities, these beams should be useful in making atom traps.

This work was supported by The Research Corporation, Digital Optics Corporation, and the University of Oklahoma.

[1] H. He, M. E. J. Friese, N. R. Heckenberg, and H. Rubinsztein-Dunlop, Phys. Rev. Lett. **75**, 826 (1995).
[2] L. Aterson, M. P. MacDonald, W. S. J. Arlt, P. E. Bryant, and K. Dholakia, Science **292**, 912 (2001).
[3] A. G. Truscott, M. E. J. Friese, N. R. Heckenberg, and H. Rubinsztein-Dunlop, Phys. Rev. Lett. **82**, 1438 (1999).
[4] D. Rozas, C. T. Law, and G. A. Swartzlander, Jr., J. Opt. Soc. Am. B **14**, 3054 (1997).
[5] M. J. Snadden, A. S. Bell, R. B. M. Clarke, E. Riis, and D. H. McIntyre, J. Opt. Soc. Am. B **14**, 544 (1997).
[6] T. Kuga, Y. Torii, N. Shiokawa, T. Hirano, Y. Shimizu, and H. Sasada, Phys. Rev. Lett. **78**, 4713 (1997).
[7] E. M. Wright, J. Arlt, and K. Dholakia, Phys. Rev. A **63**, 013608 (2001).
[8] J. Tempere, J. T. Devreese, and E. R. I. Abraham, Phys. Rev. A **64**, 023603 (2001).
[9] A. E. Siegman, Lasers (University Science Books, Mill Valley, CA, 1986).
[10] L. Allen, M. W. Beijersbergen, R. J. C. Spreeuw, and J. P. Woerdman, Phys. Rev. A **45**, 8185 (1992).
[11] M. Harris, C. A. Hill, and J. M. Vaughan, Opt. Commun. **106**, 161 (1994).
[12] E. Abramochkin and V. Volostnikov, Opt. Commun. **83**, 123 (1991).
[13] G. A. Turnbull, D. A. Robertson, G. M. Smith, L. Allen, and M. J. Padgett, Opt. Commun. **127**, 183 (1996).
[14] M. W. Beijersbergen, R. P. C. Coerwinkel, M. Kristensen, and J. P. Woerdman, Opt. Commun. **112**, 321 (1994).
[15] N. R. Heckenberg, R. McDuff, C. P. Smith, and A. G. White, Opt. Lett. **17**, 221 (1992).
[16] J. Arlt, K. Dholakia, L. Allen, and M. J. Padgett, J. Mod. Opt. **45**, 1231 (1998).
[17] M. A. Clifford, J. Arlt, J. Courtial, and K. Dholakia, Opt. Commun. **156**, 300 (1998).
[18] N. R. Heckenberg, R. McDuff, C. P. Smith, H. Rubinsztein-Dunlop, and M. J. Wegener, Opt. Quantum Electron. **24**, S951 (1992).
[19] S. N. Khonina, V. V. Kotlyar, V. A. Soifer, P. Laakkonen, and J. Turunen, Opt. Commun. **175**, 301 (2000).
[20] P. R. Bevington and D. K. Robinson, Data Reduction and Error Analysis for the Physical Sciences (McGraw-Hill, New York, 1992).